

Contents lists available at ScienceDirect

Physica B: Condensed Matter

journal homepage: www.elsevier.com/locate/physb





Detection of paramagnetic to charge-ordered insulator phase transitions in phase separated $(La_{1-\nu}Pr_{\nu})_{0.67}Ca_{0.33}MnO_3$ thin films

J.M. DeStefano a,b, A. Biswas a,*

- ^a Department of Physics, University of Florida, Gainesville, 32611, FL, USA
- ^b Department of Physics, University of Washington, Seattle, 98195, WA, USA

ARTICLE INFO

Keywords: Manganite thin films Paramagnetic insulator Charge ordered insulator Variable range hopping Adiabatic polarons

ABSTRACT

Hole-doped manganese oxides (manganites) exhibit phase separation which allows for the manipulation of phase transitions with the application of external stimuli. The three competing phases of the manganite $(La_{1-y}Pr_y)_{1-x}Ca_xMnO_3$ (LPCMO) are paramagnetic insulating (PMI), charge-ordered insulating (COI), and ferromagnetic metallic (FMM). In LPCMO thin films, the substrate induced strain often makes it difficult to distinguish between the two insulating phases (PMI and COI) using resistivity and/or magnetization measurements. Here we report a method for determining the PMI-COI transition temperature of LPCMO thin films by fitting resistance vs. temperature (R-T) data to the Arrhenius equation. This method also yields the activation energy in the COI phase which agrees with direct measurements using scanning tunneling microscopy. Analysis of the R-T data suggests that adiabatic polaron hopping is the transport mechanism in both the PMI and COI phases while variable range hopping (VRH) is the dominant mechanism in the mixed FMM/COI state.

1. Introduction

The competing magnetic and electronic phases of perovskite manganese oxides or manganites hold promise for device applications such as resistive random access memory (ReRAM) [1] as these phases can be tuned using external stimuli such as, magnetic field [2], strain [3], and electric field [4]. Manganites have also been the focus of fundamental research since they exhibit a host of exotic properties such as colossal magnetoresistance (CMR) and metal-to-insulator transitions (MIT) [2]. These phenomena are mainly caused by the competition between phases with similar free energies which form due to the interplay between spin, orbital, and lattice interactions [5-8]. Manganites can exist in three main thermodynamic phases viz. the ferromagnetic metallic (FMM), charge ordered insulator (COI), and paramagnetic insulator (PMI) phases [3]. The competition for thermodynamic stability among these three phases can be tuned using parameters such as chemical composition [9-12], temperature [3], and magnetic field [13], which leads to the rich phase diagram of manganites and their sensitivity to external perturbations. The PMI phase is stable at higher temperatures [13,3]. As the temperature is lowered there is usually a second order transition to FMM or COI depending on the specific chemical composition of the material. For example, in Nd_{0.5}Sr_{0.5}MnO₃, there is a phase transition from PMI to FMM phase on cooling [14]

while, in $Pr_{0.5}Sr_{0.5}MnO_3$, there is a transition from PMI to COI phase on cooling [15]. The FMM or COI phase thus obtained may remain thermodynamically stable down to the lowest temperatures [15] or undergo a transition to a COI or FMM phase, respectively [14]. The FMM-COI transition is first order in nature which can lead to coexistence of these two phases in manganites such as $(La_{1-y}Pr_y)_{1-x}Ca_xMnO_3$ (LPCMO), which has been observed using various microscopy techniques [16]. This phase separation has been studied extensively, both in order to understand and manipulate the interplay between these two phases [17,18]. At low temperatures, the phase competition leads to a strain-glass [19] or spin-glass [12] behavior which gives way to dynamic phase separation at higher temperatures [19,20].

The first order transition between the FMM and COI phases is easy to detect using measurements such as resistivity or magnetization as a function of temperature since the COI phase has high resistivity and low magnetization while the FMM phase has low resistivity and high magnetization [14]. The second order transition from PMI to FMM is also easy to detect since the PMI phase has a low magnetization and the associated insulator-to-metal transition can be observed clearly using resistivity measurements [14]. However, in materials which show a PMI to COI second order transition, the change in resistivity and/or magnetization may be difficult to detect since both phases

E-mail addresses: jdest@uw.edu (J.M. DeStefano), amlan@phys.ufl.edu (A. Biswas). URL: http://www.phys.ufl.edu/~amlan/ (A. Biswas).

^{*} Corresponding author.

are insulating and have low magnetization. Such a scenario occurs in compounds such as Pr_{0.7}Ca_{0.3}MnO₃ [21] and LPCMO [22]. The problem with detecting the PMI-COI transition is exacerbated in thin films due to substrate induced strain which suppresses the associated structural transition [23]. Determining this phase transition in thin film manganites requires sophisticated techniques since heat capacity measurements are not possible. Many of these studies are based on finding a slight change to the crystal lattice; for example, polarized optical microscopy [24] and transmission electron microscopy [25] have been utilized in these efforts. Here we report a method for detecting the PMI to COI phase transition in LPCMO thin films grown on (110) NdGaO3 (NGO) substrates using resistivity measurements, which takes advantage of the different origins of insulating behavior in the two phases. The resistance vs. temperature (R - T) behavior of the COI phase suggests that an energy gap in the density of states leads to insulating behavior while the PMI phase is insulating due to large Jahn-Teller polaronic fluctuations [26]. Both mechanisms lead to activated resistivity behavior but with different activation energies. We measured the activation energies for LPCMO thin films by fitting the R-T curves to the Arrhenius equation. The temperature at which the activation energy changes is then designated as the transition temperature between the PMI and COI phases. The value of the activation energy for the COI phase found using this method agrees with prior measurements of charge ordering energy gaps using scanning tunneling spectroscopy [27]. We also measure the effect of an external magnetic field and a change in chemical composition on the activation energies and phase transitions. This method is remarkably simpler to employ than the microscopy techniques listed above for extracting the PMI-COI phase transition temperature.

2. Methods

30 nm thick $(La_{1-y}Pr_y)_{1-x}Ca_xMnO_3$ thin films with y=0.5 (LP5) and 0.6 (LP6) (both with x=0.33) were grown on (110) NGO substrates using pulsed laser deposition. The details of the synthesis and characterization of the samples can be found elsewhere [3,28]. Magnetotransport properties were measured in a commercial cryostat with a reading being taken every 2 K from 20–300 K. A two-probe method was used for resistance measurements with a constant voltage source set to 10 V and a 1 M Ω resistor in series with the sample. This method is outlined in Ref. [9]. Four-probe measurements at higher temperatures matched the two-probe measurements which confirmed the negligible effect of contact resistance. However, four-probe measurements were not feasible at low temperatures due to the high samples resistances, which are comparable to the input impedance of the voltmeters. Magnetization measurements were taken using a Quantum Design MPMS.

3. Experimental results

3.1. Growth of FMM regions

Fig. 1a shows the R-T data for the LP6 thin film. The usual features of MIT, CMR, and thermal hysteresis are observed. A sharp drop in R is observed in the warming run at low temperatures for both the 0 and 1 T data. This drop in resistance is due to a low temperature strain glass phase observed in phase separated and charge-ordered manganites [19,12]. At zero applied magnetic field, a small "shoulder" can be seen around 112 K, which is suppressed as the external field is increased. The inset shows this trend over a smaller temperature range for more magnetic fields. The shoulder is marked with an arrow for clarity. If this shoulder is due to the PMI to COI transition, the shoulder should move to lower temperatures in an applied magnetic field. To determine whether if this feature was indeed shifting in temperature as a function of magnetic field, a numerical derivative of the $\ln(R)$ with respect to temperature was taken for the low field data (Fig. 1b).

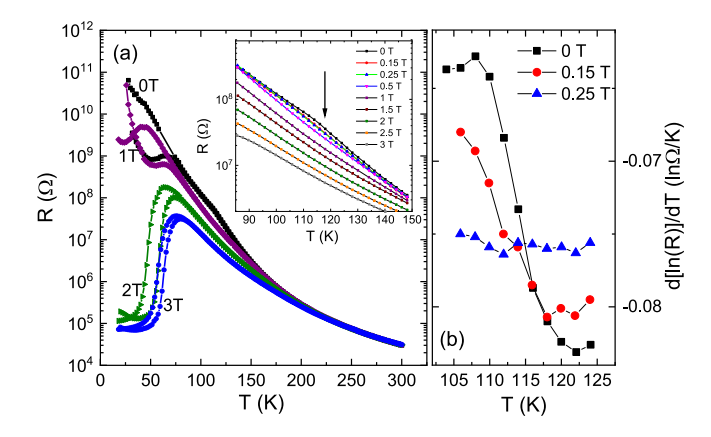


Fig. 1. (a). R-T data for LP6 at different magnetic fields. A "shoulder" feature (marked with an arrow) is observed at 112 K and a magnified view is shown in the inset. (b). The numerical derivative of $\ln(R)$ with respect to T for LP6.

To reduce noise, this derivative was obtained using a standard fivepoint, unweighted smoothing process. As a higher field is applied, the derivative gets flatter, indicating that the feature is going away. This analysis shows that the shoulder's temperature does not change significantly (within the 2K separation between data points) before being completely suppressed, which suggests that the shoulder feature is not due to the PMI to COI transition. Low-field magnetization measurements (100 Oe) on similar thin film LP6 samples show a clear rise in the magnetization at roughly this temperature which was identified as the Curie temperature (T_C) (data from Ref. [3] shown in inset of Fig. 2), leading to the conclusion that the shoulder in the magnetotransport data is indicative of the initial formation of the FMM regions in the COI background upon cooling leading to a slight suppression in resistance and the shoulder feature. As the magnetic field is increased, the FMM phase free energy is lowered and the COI phase breaks down causing this phase transition to occur at a higher temperature as has been shown earlier in single crystals of $Pr_{1-x}Ca_xMnO_3$ [29].

The FMM phase has a lower free energy in LP5 than in LP6 due to the lower Pr content, leading to an MIT at a higher temperature as shown in Fig. 2 [9]. However, magnetization data (with the background of the paramagnetic substrate removed using Curie's law) of LP5 suggest that the nucleation of FMM regions at zero external magnetic field occurs at roughly the same temperature as in LP6 (Fig. 2, inset). This magnetization behavior implies that the FMM regions that grow in are initially larger for LP5 than those in LP6, as has been observed using spin-polarized neutron reflectometry [30,31]. The larger initial size of the FMM regions in LP5 leads to a smaller temperature difference between the initial formation of FMM regions and the MIT due to percolation compared to LP6. Hence, there is no observable shoulder in the R-T data as the large resistance change due to the MIT obscures the relatively small resistance change caused by the initial nucleation of the FMM regions. Therefore, for both LP5 and LP6, the R-T data does not show a clear signature of the PMI-COI phase transition and a more detailed analysis of the data is needed to extract the PMI-COI transition temperature.

3.2. PMI to COI phase transition

Previous analyses of the transport properties of the insulating states in manganites have been carried out using various fitting functions [32] and we found that an Arrhenius equation of the form

$$R = R_0 e^{\frac{E_A}{k_B T}} \tag{1}$$

(where E_A is an activation energy for a particular insulating phase) provided good fits at each field strength for our magnetotransport

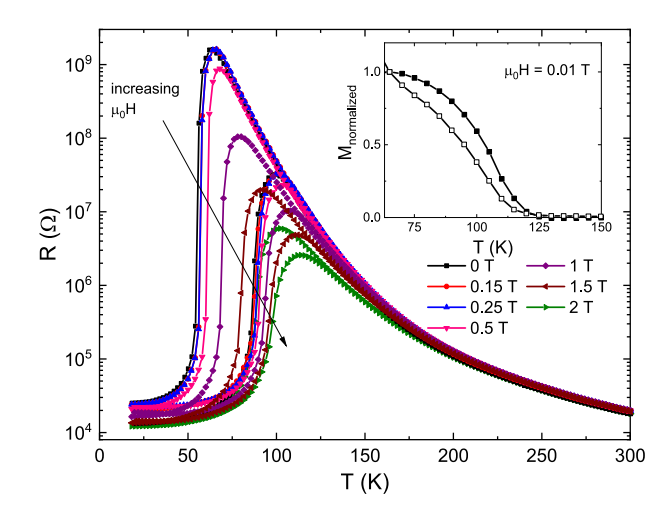


Fig. 2. R-T data for LP5 at different magnetic fields. Inset: Magnetic moment as a function of temperature for LP5 (filled squares) and LP6 (open squares, data for LP6 taken from Ref. [3]). The magnetic contributions of the paramagnetic substrates were removed using Curie's law.

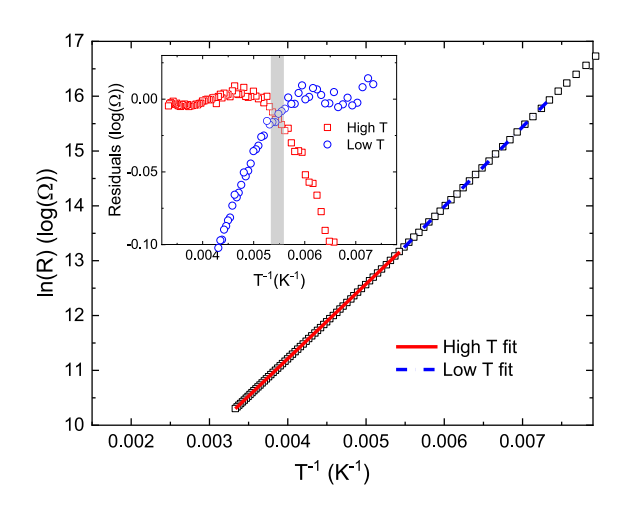


Fig. 3. An example of the two linear fits to the R-T data for LP6 with no applied magnetic field. The quality of fit here is typical of that achieved using our methodology. Inset: Residuals of the fits. Note that the residuals are relatively small in the range in which the fits are valid. The gray shaded area shows the estimated PMI-COI transition region.

data at temperatures above the MIT. Using Eq. (1) we will now show that there are two distinct regions in the R-T data with different fitting parameters and that these two regions correspond to the PMI (at higher temperature) and COI (at lower temperature) phases. In order to determine where to switch from the high temperature to low temperature fit, the following steps were taken: (1) a linear fit was performed on the $\ln R$ vs. 1/T data from the highest temperature of 300 K down to temperatures where a visual inspection showed the residuals deviating from zero, (2) then points were removed one-by-one from the low temperature side of the fit until a point was found that was local minimum in $|1 - R^2|$. The same steps were taken with the low temperature fit, except that the highest temperature for this fit was the one 2 K below the lowest temperature of the higher temperature fit. The fits obtained using this method are shown in Fig. 3 for R-T data in zero magnetic field. The residuals of these fits are shown in the inset of the figure. The residuals are relatively small in the range these fits have been determined to be valid. The gray shaded area shows the estimated PMI-COI transition region. Hence, using this method we find that the PMI to COI transition occurs at 185 \pm 3 K during cooling.

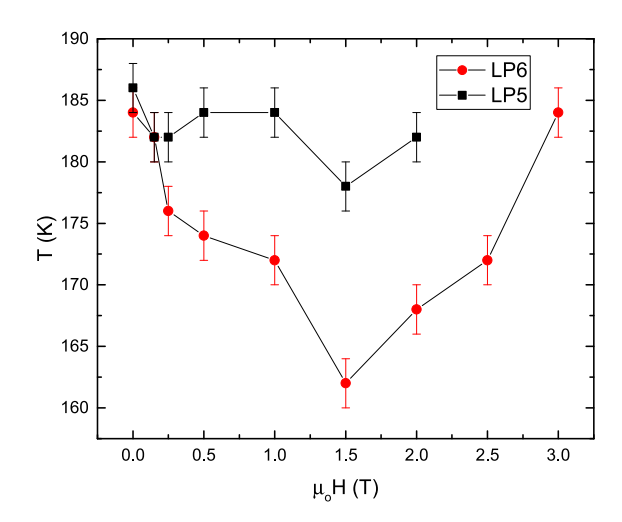


Fig. 4. The PMI-COI transition temperature as a function of applied field for LP6 and LP5 $\,$

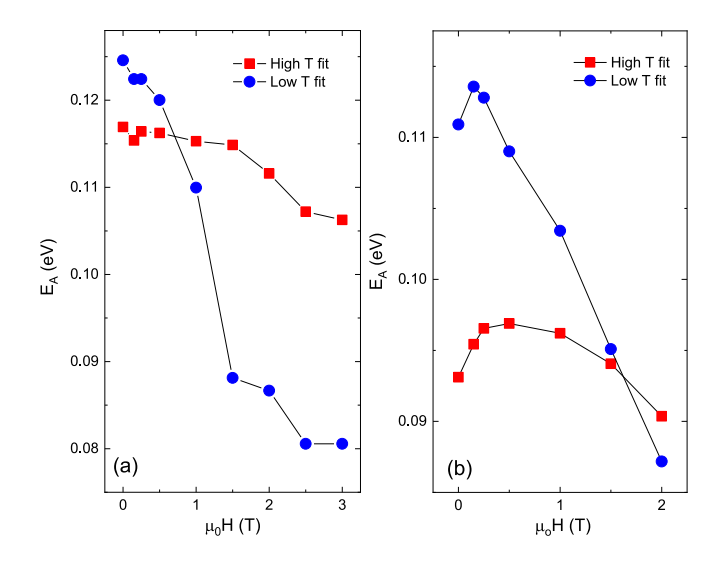


Fig. 5. The activation energy E_A as a function of field for LP6 (a) and LP5 (b). The high temperature fit refers to the PMI phase, and the low temperature fit refers to either a purely COI phase or a mixed COI/FMM phase depending on the applied field (see main text).

In addition to the PMI to COI transition temperatures (Fig. 4, red), fits of the LP6 data also yield activation energy (E_A) values as shown in Fig. 5a. The E_A s obtained for the COI phase agree with the charge ordering gap values obtained from previous scanning tunneling spectroscopy measurements [27]. Fig. 4 also shows that the PMI to COI transition temperature is lowered when a magnetic field is applied, an effect which has been observed before in manganite single crystals with a PMI-COI phase transition [33]. However, the transition temperatures start rising above 1.5T which is likely due to the encroachment of the FMM phase. The free energy of the FMM phase drops as higher external fields are applied leading to the formation of FMM regions at higher temperatures and a collapse of the COI phase [29]. The E_A values obtained from the low temperature fits agree with this assessment showing a rapid decrease until $\approx 1.5\,\mathrm{T}$ and a subsequent slower decrease as shown in Fig. 5. The activation energy of the high temperature fit (PMI phase) is relatively unchanged with an increasing magnetic field. Hence, we conclude that for $H \ge 1.5 \,\mathrm{T}$, the transition temperatures obtained from our fitting method reveal a PMI to a mixed FMM and COI phase transition (instead of a PMI to pure-COI transition), which indeed occurs at higher temperatures for increasing magnetic fields.

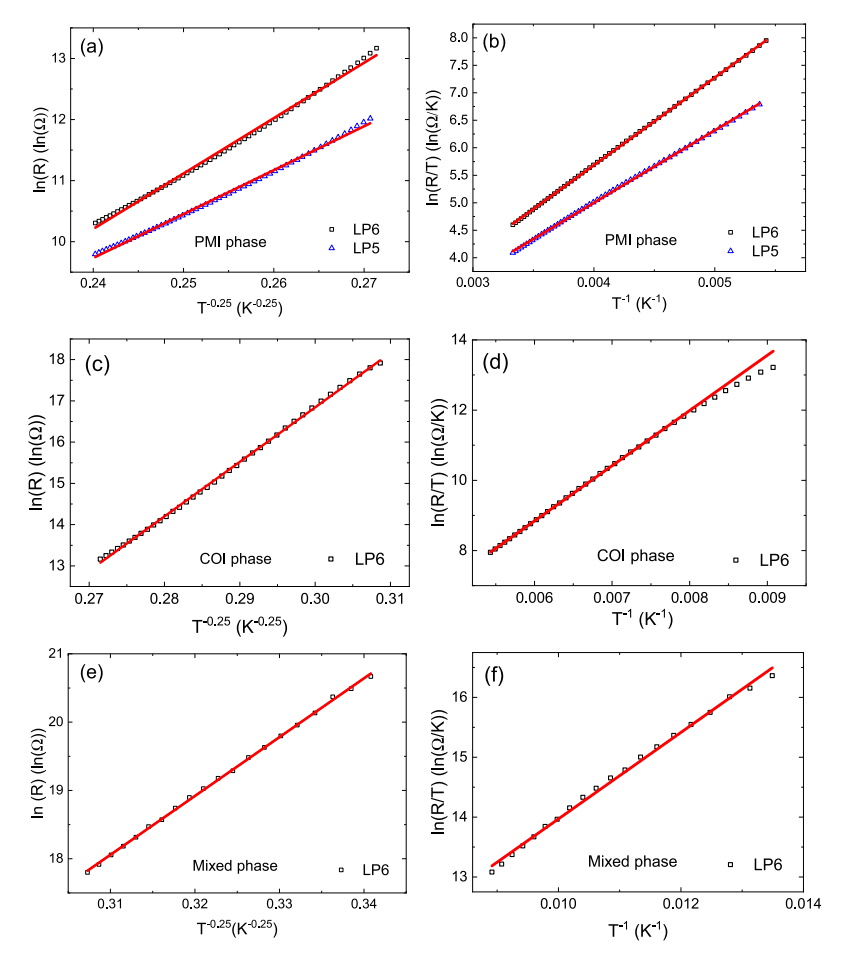


Fig. 6. Fits to the variable range hopping ((a), (c), and (e)) and adiabatic polaron hopping ((b), (d), and (f)) for temperatures ranges corresponding to the PMI, COI, and mixed phase states. The COI phase and the mixed phase state are shown only for the LP6 sample. The adjusted R^2 values for each fit are shown in Table 1.

The fits of the LP5 data yield PMI transition temperatures (Fig. 4, black squares) and activation energies (Fig. 5b) which need a different explanation from the LP6 data due to the increased metallicity of LP5. The change in the PMI to COI transition temperature is small, essentially within the error bar of our method. The activation energy values are also smaller compared to LP6 and, while the trend with an applied magnetic field is similar to LP6, the overall change is smaller. Hence, our method gives values for the PMI to COI transition temperature and their activation energies in LP5 which are similar to LP6 (186 \pm 2 K and 0.11 eV, respectively) at zero magnetic field. However, the lower free energy of the FMM phase in LP5 prevents us from using this method to determine the variation of the transition temperature and energy gap as a function of magnetic field.

3.3. Transport models for the insulating phases

We further assessed the validity of our method by checking if the PMI to COI transition temperatures, determined using fits to Eq. (1), were compatible with other widely used transport models for the PMI and COI phases. First, we fit the PMI R-T data for LP5 and LP6 at zero applied field to a variable range hopping (VRH) model of the form

$$\ln\left[\frac{R(T)}{R_{\infty}}\right] = \left(\frac{T_0}{T}\right)^{0.25} \tag{2}$$

where R_{∞} depends on the phonon density and T_0 depends on the localization length of the electrons and the density of states [32]. As opposed to a nearest neighbor hopping model, the VRH model takes into account the fact that a hopping electron will try to find the lowest activation energy of hopping and the shortest possible hopping distance [34].

Generically these conditions are not simultaneously satisfied by the nearest neighbor, and instead the electron hops an optimum distance to fit these criteria as best as possible. As the temperature of the system changes, this optimum distance also changes, bringing about the name of the model. The fits to our data are shown in Fig. 6(a), and the adjusted R^2 for LP6 and LP5 are 0.99738 and 0.99822 respectively (see Table 1). The deviation of the best fit line from the data is clear and consistent in both compounds: the high and low temperature regions of the PMI phase are underpredicted and the middle temperatures are overpredicted. Alternatively, the adiabatic polaron hopping model [35] of the form shown in Eq. (3)

$$R = BTe^{\frac{E_a}{k_B T}} \tag{3}$$

has had success in the modeling of similar materials, including the PMI phase of $La_{0.67}Ca_{0.33}MnO_3$ [36]. This model produces better fits to our data as shown in Fig. 6(b). The adjusted R^2 for LP6 and LP5 are 0.99993 and 0.99970, respectively (Table 1) and the residuals do not have a distinct shape. Hence, the polaron hopping model is the likely mechanism for insulating behavior in the paramagnetic phase of LPCMO. We also fitted the LP6 R-T data for temperatures below the PMI to COI transition temperature (extracted using our method) but above the shoulder feature seen in Fig. 1(a). In this temperature range the LP6 sample is expected to be in a pure COI state. Fits to the VRH and polaron hopping models for this temperature range are shown in Fig. 6(c) and (d), respectively. The polaron hopping model provides a slightly better fit for this temperature range with an adjusted R^2 value of 0.99984 while the VRH model gives an adjusted R^2 of 0.99930 (Table 1).

Table 1 Adjusted R^2 values for the fits shown in Fig. 6. The bold values denote the prevalent transport mechanism (adiabatic polaron (AP) or variable range hopping (VRH)) for the corresponding phase.

Phase	Transport mechanism	
	VRH	AP
LP5 (PMI)	0.99822	0.99970
LP6 (PMI)	0.99738	0.99993
LP6 (COI)	0.99930	0.99984
LP6 (mixed)	0.99932	0.99618

At temperatures below the shoulder feature of LP6 shown in Fig. 1(a), there is a mixed phase state due to the coexistence of the FMM and COI phases. We fitted the data for temperatures between T_{MI} and the shoulder feature of LP6 to the VRH and adiabatic polaron models as shown in Fig. 6(e) and (f). For this temperature range, the adjusted R^2 for the adiabatic polaron model is 0.99618 but it is the VRH model that produces a better fit with an adjusted R^2 of 0.99932. The corresponding value of T_0 obtained from the VRH fit is 5.5×10^7 K which is similar to the values obtained for La_{0.7}Ca_{0.3}MnO₃ [32]. The good fit to the VRH model in this temperature range may be due to coexistence of the FMM and COI phases as suggested in Ref. [37].

4. Conclusions

We have shown that the PMI to COI phase transition can be detected using the R-T data for LPCMO thin films grown on NGO by fitting the data to the Arrhenius equation. The fits also provide the activation energies for the two phases. The value of the activation energy for the COI phase agrees with direct measurements using scanning tunneling microscopy. The application of a magnetic field lowers the PMI to COI transition temperature. A further increase in the magnetic field causes the growth of FMM regions at higher temperatures, allowing for direct competition between the FMM and PMI phases at high magnetic fields. Fits of the R-T data to the VRH and adiabatic polaron hopping models suggest that adiabatic polaron hopping is at play in both the PMI and COI phases while VRH is the dominant mechanism in the mixed FMM/COI state. Future work could be done with different substrates to explore how the COI phase is impacted by different amounts of lattice strain.

CRediT authorship contribution statement

J.M. DeStefano: Experiment design, Transport measurements, Data analysis, Writing – original draft. **A. Biswas:** Conceptualization, Writing – original draft.

Declaration of competing interest

The authors declare that they have no known competing financial interests or personal relationships that could have appeared to influence the work reported in this paper.

Data availability

Data will be made available on request.

Acknowledgments

Work on this project was supported by the National Science Foundation (NSF), United States via DMR-1852138 and DMR-1410237.

References

- [1] T. Fujii, H. Kaji, H. Kondo, K. Hamada, M. Arita, Y. Takahashi, IOP Conf. Ser. Mater. Sci. Eng. 8 (2010) 012033, http://dx.doi.org/10.1088/1757-899X/8/1/012033, URL https://iopscience.iop.org/article/10.1088/1757-899X/ 8/1/012033.
- [2] P.K. Siwach, H.K. Singh, O.N. Srivastava, J. Phys.: Condens. Matter 20 (27) (2008) 273201, http://dx.doi.org/10.1088/0953-8984/20/27/273201, URL https://iopscience.iop.org/article/10.1088/0953-8984/20/27/273201.
- [3] Hyoungjeen Jeen, Amlan Biswas, Phys. Rev. B 83 (6) (2011) 064408, http://dx.doi.org/10.1103/PhysRevB.83.064408, URL https://link.aps.org/doi/ 10.1103/PhysRevB.83.064408.
- [4] Ambika Shakya, Amlan Biswas, J. Appl. Phys. 127 (21) (2020) 213902, http://dx.doi.org/10.1063/5.0004862, URL http://aip.scitation.org/doi/10.1063/5.0004862
- [5] Clarence Zener, Phys. Rev. 82 (1951) 403–405, URL https://link.aps.org/doi/10. 1103/PhysRev.82.403.
- [6] Z. Jirak, Z. Krupicka, S. Simsa, M. Dlouha, S. Vratislav, J. Magn. Magn. Mater. 53 (1985) 153, http://dx.doi.org/10.1016/0304-8853(85)90144-1.
- [7] A.J. Millis, Nature 392 (1998) 147, http://dx.doi.org/10.1038/32348.
- [8] K.H. Ahn, T. Lookman, A.R. Bishop, Nature 428 (6981) (2004) 401–404, http://dx.doi.org/10.1038/nature02364, URL http://www.nature.com/doifinder/10.1038/nature02364.
- [9] Tara Dhakal, Jacob Tosado, Amlan Biswas, Phys. Rev. B 75 (9) (2007) 092404, http://dx.doi.org/10.1103/PhysRevB.75.092404, URL https://link.aps.org/doi/10.1103/PhysRevB.75.092404.
- [10] P. Schiffer, A.P. Ramirez, W. Bao, S.-W. Cheong, Phys. Rev. Lett. 75 (18) (1995) 3336–3339, http://dx.doi.org/10.1103/PhysRevLett.75.3336.
- [11] Mintu Debnath, Esa Bose, Sudipta Pal, J. Magn. Magn. Mater. 575 (2023) 170752, http://dx.doi.org/10.1016/j.jmmm.2023.170752.
- [12] Mintu Debnath, Bhaskar Biswas, Esa Bose, Sambhu Charan Das, Souvik Chatterjee, Sudipta Pal, J. Alloys Compd. 921 (2022) 166048, http://dx.doi.org/10.1016/j.jallcom.2022.166048.
- [13] H. Kuwahara, Y. Tomioka, A. Asamitsu, Y. Moritomo, Y. Tokura, Science 270 (5238) (1995) 961–963, http://dx.doi.org/10.1126/science.270.5238.961, URL https://www.sciencemag.org/lookup/doi/10.1126/science.270.5238.961.
- [14] R. Rawat, K. Mukherjee, Kranti Kumar, A. Banerjee, P. Chaddah, J. Phys.: Condens. Matter 19 (25) (2007) 256211, http://dx.doi.org/10.1088/0953-8984/19/25/256211, URL https://iopscience.iop.org/article/10.1088/0953-8984/19/25/256211.
- [15] Z. Jirák, E. Hadová, O. Kaman, K. Knížek, M. Maryško, E. Pollert, M. Dlouhá, S. Vratislav, Phys. Rev. B 81 (2) (2010) 024403, http://dx.doi.org/10. 1103/PhysRevB.81.024403, URL https://link.aps.org/doi/10.1103/PhysRevB.81. 024403.
- [16] L. Zhang, C. Israel, A. Biswas, R.L. Greene, A. de Lozanne, Science 298 (5594) (2002) 805–807, http://dx.doi.org/10.1126/science.1077346, URL https://www.sciencemag.org/lookup/doi/10.1126/science.1077346.
- [17] T.Z. Ward, J.D. Budai, Z. Gai, J.Z. Tischler, Lifeng Yin, J. Shen, Nat. Phys. 5 (12) (2009) 885–888, http://dx.doi.org/10.1038/nphys1419.
- [18] N.S. Bingham, P. Lampen, M.H. Phan, T.D. Hoang, H.D. Chinh, C.L. Zhang, S.W. Cheong, H. Srikanth, Phys. Rev. B 86 (6) (2012) 064420, http://dx.doi.org/10.1103/PhysRevB.86.064420.
- [19] P.A. Sharma, Sung Baek Kim, T.Y. Koo, S. Guha, S.-W. Cheong, Phys. Rev. B 71 (2005) 224416, http://dx.doi.org/10.1103/PhysRevB.71.224416.
- [20] Worasom Kundhikanjana, Zhigao Sheng, Yongliang Yang, Keji Lai, Eric Yue Ma, Yong-Tao Cui, Michael A. Kelly, Masao Nakamura, Masashi Kawasaki, Yoshinori Tokura, Qiaochu Tang, Kun Zhang, Xinxin Li, Zhi-Xun Shen, Phys. Rev. Lett. 115 (2015) 265701, http://dx.doi.org/10.1103/PhysRevLett.115.265701, URL https://link.aps.org/doi/10.1103/PhysRevLett.115.265701.
- [21] J. Barratt, M.R. Lees, G. Balakrishnan, D. McK Paul, Appl. Phys. Lett. 68 (3) (1996) 424–426, http://dx.doi.org/10.1063/1.116721, URL http://aip.scitation.org/doi/10.1063/1.116721.
- [22] M. Uehara, S. Mori, C.H. Chen, S.-W. Cheong, Nature 399 (6736) (1999) 560–563, http://dx.doi.org/10.1038/21142, URL http://www.nature.com/articles/21142.
- [23] Harsh Bhatt, Yogesh Kumar, C.L. Prajapat, M.K. Thota, Surendra Singh, Bull. Mater. Sci. 42 (6) (2019) 267, http://dx.doi.org/10.1007/s12034-019-1941-y, URL http://link.springer.com/10.1007/s12034-019-1941-y.
- [24] V. Podzorov, B.G. Kim, V. Kiryukhin, M.E. Gershenson, S.-W. Cheong, Phys. Rev. B 64 (14) (2001) 140406, http://dx.doi.org/10.1103/PhysRevB.64.140406, URL https://link.aps.org/doi/10.1103/PhysRevB.64.140406.
- [25] J. Tao, K. Sun, W.-G. Yin, L. Wu, H. Xin, J.G. Wen, W. Luo, S.J. Pennycook, J.M. Tranquada, Y. Zhu, Sci. Rep. 6 (1) (2016) 37624, http://dx.doi.org/10. 1038/srep37624.
- [26] N.D. Mathur, P.B. Littlewood, Solid State Commun. 119 (4–5) (2001) 271–280, http://dx.doi.org/10.1016/S0038-1098(01)00112-0, URL http://arxiv.org/abs/cond-mat/0104238 arXiv: cond-mat/0104238.
- [27] J.Q. He, V.V. Volkov, T. Asaka, S. Chaudhuri, R.C. Budhani, Y. Zhu, Phys. Rev. B 82 (22) (2010) 224404, http://dx.doi.org/10.1103/PhysRevB.82.224404, URL https://link.aps.org/doi/10.1103/PhysRevB.82.224404.

- [28] Hyoungjeen Jeen, Rafiya Javed, Amlan Biswas, Appl. Phys. A 122 (2016) 35, http://dx.doi.org/10.1007/s00339-015-9543.
- [29] Y. Tomioka, A. Asamitsu, H. Kuwahara, Y. Moritomo, Y. Tokura, Phys. Rev. B 53 (4) (1996) R1689(R), http://dx.doi.org/10.1103/PhysRevB.53.R1689.
- [30] Surendra Singh, M.R. Fitzsimmons, T. Lookman, J.D. Thompson, H. Jeen, A. Biswas, M.A. Roldan, M. Varela, Phys. Rev. Lett. 108 (2012) 077207, http://dx.doi.org/10.1103/PhysRevLett.108.077207, URL https://link.aps.org/doi/10.1103/PhysRevLett.108.077207.
- [31] Surendra Singh, J.W. Freeland, M.R. Fitzsimmons, H. Jeen, A. Biswas, Sci. Rep. 6 (2016) 29632, http://dx.doi.org/10.1038/srep29632.
- [32] M. Viret, L. Ranno, J.M.D. Coey, J. Appl. Phys. 81 (8) (1997) 4964–4966, http://dx.doi.org/10.1063/1.365013, URL http://aip.scitation.org/doi/10.1063/1.365013.
- [33] M. Tokunaga, N. Miura, Y. Tomioka, Y. Tokura, Phys. Rev. B 57 (9) (1998) 5259, http://dx.doi.org/10.1103/PhysRevB.57.5259.
- [34] Dong Yu, Congjun Wang, Brian L. Wehrenberg, Philippe Guyot-Sionnest, Phys. Rev. Lett. 92 (21) (2004) 216802, http://dx.doi.org/10.1103/PhysRevLett.92. 216802
- [35] David Emin, T. Holstein, Ann. Physics 53 (3) (1969) 439–520, http://dx.doi.org/ 10.1016/0003-4916(69)90034-7, URL https://www.sciencedirect.com/science/ article/pii/0003491669900347.
- [36] D.C. Worledge, G. Jeffrey Snyder, M.R. Beasley, T.H. Geballe, Ron Hiskes, Steve DiCarolis, J. Appl. Phys. 80 (9) (1996) 5158–5161, http://dx.doi.org/10.1063/ 1.363498, URL http://aip.scitation.org/doi/10.1063/1.363498.
- [37] Yu.Kh. Vekilov, Ya.M. Mukovskii, Solid State Commun. 152 (13) (2012) 1139, http://dx.doi.org/10.1016/j.ssc.2012.04.001.